

PCCP

Accepted Manuscript



This is an *Accepted Manuscript*, which has been through the Royal Society of Chemistry peer review process and has been accepted for publication.

Accepted Manuscripts are published online shortly after acceptance, before technical editing, formatting and proof reading. Using this free service, authors can make their results available to the community, in citable form, before we publish the edited article. We will replace this *Accepted Manuscript* with the edited and formatted *Advance Article* as soon as it is available.

You can find more information about *Accepted Manuscripts* in the [Information for Authors](#).

Please note that technical editing may introduce minor changes to the text and/or graphics, which may alter content. The journal's standard [Terms & Conditions](#) and the [Ethical guidelines](#) still apply. In no event shall the Royal Society of Chemistry be held responsible for any errors or omissions in this *Accepted Manuscript* or any consequences arising from the use of any information it contains.

Origin of Ion Selectivity at the Air/Water Interface

Cite this: DOI: 10.1039/x0xx00000x Lu Sun^a, Xin Li^a, Yaoquan Tu^a, Hans Ågren^a *

Received 00th January 2014,
Accepted 00th January 2014

DOI: 10.1039/x0xx00000x

www.rsc.org/

ABSTRACT. Among many characteristics of ions, their capability to accumulate at air/water interfaces is a particular issue that has been the subject of much research attention. For example, the accumulation of halide anions (Cl⁻, Br⁻, I⁻) at the water surface is of great importance for heterogeneous reactions that are of environmental concern. However, the actual mechanism that drives anions towards the air/water interface remains unclear. In this work, we have performed atomistic simulations using polarizable models to mimic ionic behavior under atmospheric conditions. We find that larger anions are abundant at the water surface and that the cations are pulled closer to the surface by the counterions. We propose that polarization effects stabilize the anions with large radii when approaching to the surface. This energetically more favorable situation is caused by that the more polarized anions at the surface attract water molecules more strongly. Of relevance is also the ordering of the surface water molecules with their hydrogen atoms pointing outwards which induce an external electronic field that leads to different surface behavior of anions and cations. The water-water interaction is weakened by the distinct water-ion attraction, a point contradicting the proposition that F⁻ is a kosmotrope. The simulation results thus allow us to obtain a more holistic understanding of the interfacial properties of ionic solutions and atmospheric aerosols.

1. Introduction

The nature of ions at the air/water interface has long been a topic of intensive studies. The predominant Onsager and Samaras theory and Gibbs adsorption isotherm from the last century assert that mono-atomic ions are repelled from the surface by their image charge and reach the bulk as the energetically more favorable situation.¹ However, a decade ago it was predicted by molecular dynamics simulations that halide anions (Cl⁻, Br⁻, I⁻) remain at the interface.² The surface-excessive propensities of Br⁻ and I⁻ have also been corroborated by state-of-the-art experiments.³ This intriguing ion specificity reinvigorates the discussion of electrolyte solutions due to the vital effects of ions on atmospheric-relevant phenomena. For instance, oxidation of larger halide anions within sea-salt aerosols is found to be responsible for ozone depletion in remote Arctic areas while their surface adsorption would appreciably increase the probabilities of heterogeneous reactions.⁴ Moreover, the sequence of surface-affinity, F⁻ < Cl⁻ < Br⁻ < I⁻, coincides with the reversed Hofmeister series, which arises from experimental findings that the former ions in this series have a salting-out effect of proteins while the latter ions have a salting-in effect.⁵ This further implies a complex interaction between ions and organic debris in atmospheric

aerosols.⁶ Nevertheless, the mechanism governing the ion specificity remains mysterious. Interpretations have been made by classifying ions into two categories, i.e. kosmotropic (structure making) and chaotropic (structure breaking), a classification that though remains controversial.⁷ A wealth of relevant experiments has been conducted to validate the interfacial enhancement of halide anions and to study their features, often together with alkali cations. Vibrational sum-frequency generation combined with Raman spectra supports the positive enhancement of Br⁻ and I⁻ on the surface because the noncentrosymmetric interface extends deeper into the bulk of their solutions compared to pure water.^{3d} X-ray photoelectron spectroscopy has been further utilized to analyse the anion/cation rate during salts deliquesce, which shows a rising trend from bulk to surface for Br⁻ and I⁻.⁸ NMR relaxation studies have shown that Li⁺, Na⁺, K⁺ and F⁻ enhance the hydrogen-bonded structure of water and that Cl⁻ has little influence on water structure, while other larger ions attenuate hydrogen bonds of water.^{3e, 9} Contradicting the NMR results, Raman spectroscopy indicates that only F⁻ is capable of promoting hydrogen bond creation among halide anions and alkali cations.⁹ Besides experiments, more in-depth interpretations have been accomplished at the atomic level through molecular dynamics (MD) simulations.^{3a, 3b, 10}

Pioneering MD simulations employing polarizable force fields predicted an unconventional ionic distribution that halide anions (Cl^- , Br^- , I^-) would be abundant at the surface.^{3a, 8, 11} Thus, for a long time, polarization was attributed as the driving force for the interfacial propensity. However, subsequent studies revealed the importance of charge and size of the anions by the Stockmayer liquid model and by conventional water models.^{10a, 12} More recently, free energy calculations have been performed for single ions using polarizable shell models, indicating the presence of energy traps adjacent to the air/water interface.^{3b} Furthermore, by decomposing the free energy into different contributions it has been inferred that there is a multifaceted reason why halide anions reach the surface, among which the water-water interaction is the most influential.^{3b} This point conforms to the view that structure creating and breaking is not only the result of interactions of water with the bare ions but with their surrounding water shell. Therefore, how ions are hydrated by water and in turn affect the water-water interaction has been a topic of major concern in many previous studies, mainly employing Car-Parrinello and Born-Oppenheimer types of MD simulations.^{10b, 13} Still, there is a lack of consistency among these results and an inappropriate neglect of perturbations from counterions. This necessitates a more holistic approach and an assessment of more complex systems in the investigations.

Although numerous efforts have been devoted to deciphering ion specificity at interfaces, at least two questions remain hitherto unresolved. The first one is why the later members in the anionic Hofmeister series can easily reach the surface while cations are much less abundant there.^{6, 14} Besides, alkali cations show a reversed sequence in the Hofmeister series ($\text{K}^+ > \text{Na}^+ > \text{Li}^+$) as kosmotropes.⁹ In addition, the strong electrostatic interaction between anions and cations influences the optimal position of the ions but this has been less attended. The second question is that we know that ion specificity relies on the solute, but not how water drives the ions outwards. The energetic explanation is illustrative but not comprehensive – it is still unclear how ions and water interact to induce an energy trap. The complication of the system further raises the question on how ions affect water structure, which is crucial for understanding aerosol particles. To advance our understanding beyond previous studies, we hereby present a multi-component MD simulation employing a polarizable force field to investigate the structure alteration of the whole system, and to clarify how certain ions reach the surface while others do not and how they affect the surrounding.

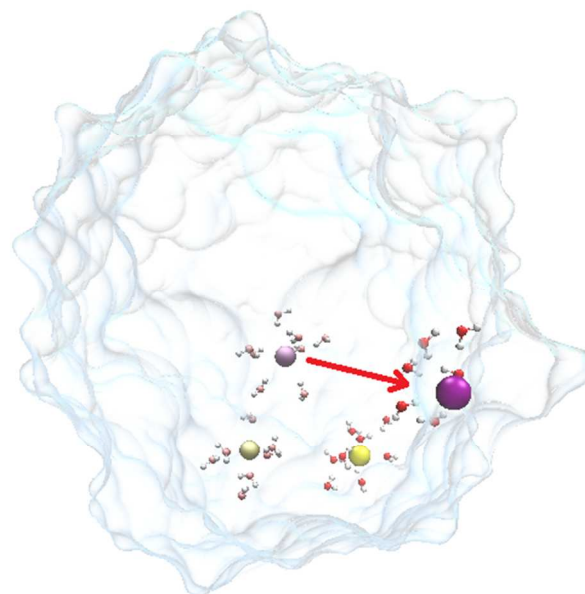
2 Computational details

Molecular dynamics simulations were carried out for a series of combinations of alkali cations and halide anions using the GROMACS package.¹⁵ The polarizable shell models for water (SWM4-DP) and ions were employed where polarization was represented by oscillating Drude particles.¹⁶ Besides conventional key parameters, an additional polarizability is included, on which iterations were based to achieve the optimal position between the real atom and the Drude particle. As we focus on the air/water interfaces, we established droplet systems which mimic aerosol shapes and possess large proportions of surface areas. Due to the expensive computations, only fixed concentrations of ions in the nano-

sized water clusters were studied, i.e. at 1.0 mol L^{-1} , and there are 1000 water molecules throughout the simulations.

To build an initial configuration, a $3.2 \times 3.2 \times 3.2 \text{ nm}$ box was first generated and followed by solvation. Ions were introduced by randomly choosing 36 water molecules and replacing them with 18 cations and 18 anions. The system was then subject to energy minimization and a short dynamics run (100 ps). In order to model a droplet (cluster), the system was placed in the center of a new box with spatial dimension $10 \times 10 \times 10 \text{ nm}^3$. Thereafter simulations were carried out under periodic boundary conditions and the NVT ensemble, which was accomplished by the Nosé-Hoover thermostat to maintain the system at room temperature (298 K).¹⁷ Water molecules were kept rigid. The long-range Coulombic interactions were recovered by the particle-mesh Ewald (PME) method with the real-space cut-off radius set at 2.5 nm.¹⁸ For each step, the Drude particle underwent iterations until the root-mean-square force was below $0.001 \text{ kJ mol}^{-1} \text{ nm}^{-1}$. Each simulation was performed for 10 ns with a time-step of 2 fs.

The free energy well of I^- at the interface was computed through umbrella samplings. I^- was first steered outwards from the center of mass of the droplet to the air/water interface within 1 ns at a speed of 2.5 nm ns^{-1} . Then 40 configurations with a time step of 25 ps were taken as initial input files for subsequent umbrella sampling simulations from the trajectory. Each umbrella sampling was performed for 4 ns and biased potential was applied with a force constant of $800 \text{ kJ mol}^{-1} \text{ nm}^{-1}$. Finally, the free energy trap for I^- residing at the interface was obtained by analysing the distribution probability through the weight histogram analysis method (WHAM).¹⁹

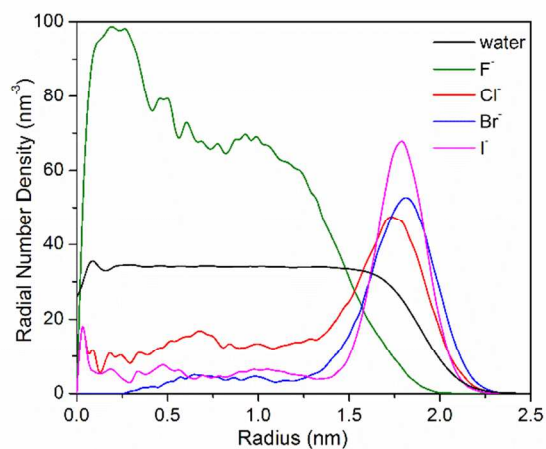


Scheme 1. Reaction path of steered MD. The purple particle denotes I^- while the yellow particle denotes Na^+ .

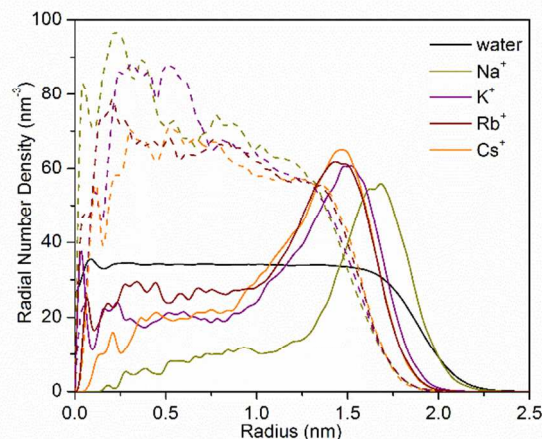
3 Results and discussion

3.1 Ion distributions

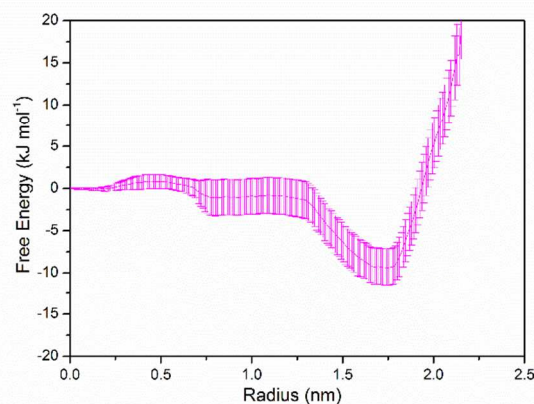
Our simulations show that ions diffuse quickly and that the average distance to the center of mass of the droplet converges within the first nanosecond. The radial number densities of a variety of combinations are plotted in Figure 1. At the radius of 1.7 nm, the water density starts to decrease and vanishes at 2.3 nm. The Gibbs dividing surface is used here to distinguish the air/water interface, which is located at about 1.95 nm to the center of mass of the droplets. Consistent with experiments, Cl^- , Br^- and I^- abound at the interface and are repelled by bulk water following the trend $\text{Cl}^- < \text{Br}^- < \text{I}^-$, while F^- moves inwards the bulk. In contrast, the cations barely reach the interface on their own and their density peaks all occur beneath the interfacial area. Small cations such as Li^+ and Na^+ are strongly attracted by anions and it is therefore probable for Li^+ to further aggregate with its counterions (Fig S1 in supporting information) while Na^+ exhibits a distribution that is more affected by its counterions compared with the larger cations. Together with I^- , Na^+ has its maximum concentration 3\AA beneath the interface while K^+ , Rb^+ and Cs^+ have their peak 5\AA below the interface. However, when we change the anion to F^- , Na^+ resides mostly inward and the differences with the other alkali cations diminish. This phenomenon accords with studies on the Hofmeister series which indicate that cations impose less effects on water structure than anions and that cations may change position in the Hofmeister series with different counterions.⁹ The ability of the large anions pulling the cations towards the interface was unravelled by free energy calculations through umbrella sampling. The free energy well for I^- near the interface is as large as -9.3 kJ mol^{-1} even in the presence of Na^+ , indicating that the energy gain of I^- at the interface is more than enough to overcome the energy increase of Na^+ near the interface.



(a)



(b)



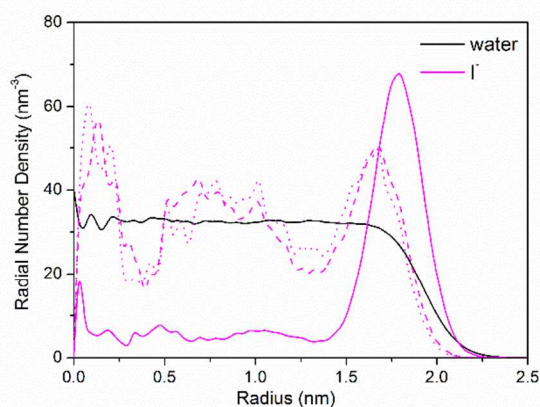
(c)

Figure 1 Radial number densities of (a) anions with Na^+ as the counterion, (b) cations with F^- (dashed line) and I^- (solid line) as the counterion, the densities of ions are rescaled by a factor of $1000/18$ in the figures. (c) The free energy by pulling I^- to the interface in the presence of Na^+ is depicted, together with the error bars.

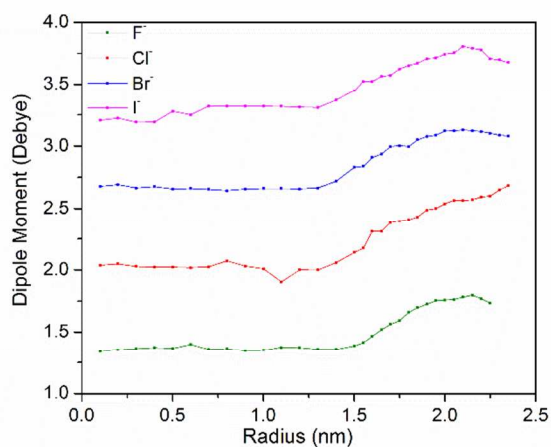
3.2 Attenuated polarizability of anions

That halide anions reside at the interface results from a combination of size, polarization, charge, and solvent effects.^{3b} However, it remains unclear what actually dominates the mechanism that pushes the anions outwards. Improved DCT model by Levin et al. has fitted the surface affinity of anions to experiments through inclusion of polarization.²⁰ But the gradually decreasing density of water at the interface differs from the simplified Gibbs dividing surface and the size alone can drive the large anions close to interface deviates from the traditional DCT model, which necessitate a further analysis by the model in this paper. We here attenuate the polarizability for the large anions in order to study how influential polarization really is. After attenuating the polarization of I^- to that of Cl^- or to 0 nm^{-3} , the anions move slightly towards bulk but the maximum density shows up only 1\AA inwards, as illustrated in Fig 2(a). In accordance with the use of conventional force

fields, the van der Waals interaction can drive the anions towards the interface.^{10a} Thus, we hypothesize that for certain big anions, size is the key to driving big anions towards the interface initially, while a more polarized configuration ascertains that certain ions are capable of adapting themselves at the interface. A further illustration is shown by the induced dipole moments of the anions in Fig 2(b). The dipole moment remains constant inside the bulk but switches to a smoothly increasing mode upon reaching the interface, implying an increase of the interaction with solvation water. Nevertheless, it is noteworthy that the polarization effect is more dominant for the smaller anion Cl^- , as shown in Fig S1(d). Reducing the polarizability of Cl^- can decrease the interfacial abundance of Cl^- ions. The result that for smaller ions the polarization effect is dominant is further verified by the outward movement of F^- after enhancing its polarizability to that of Cl^- . It is impossible for F^- to reach the same surface affinity as that of Cl^- due to the small radius of F^- .



(a)



(b)

Figure 2. (a) Polarization influences the distribution of I^- . The solid, dashed and dotted lines depicts the number densities of I^- with polarizabilities of 0.007490 nm^{-3} , 0.003969 nm^{-3} and 0 nm^{-3} , respectively. (b) Induced dipole moments of anions adjust according to position. The anions become more polarized from radius equals to 1.5 nm , from where larger anions start to accumulate.

3.3 Hydration structure of ions

The high hydration energies of halide anions reported are conventionally thought to be sufficient to overcome the cost of inserting ions into water by creating a cavity, a property being called stiffness.⁹ Nevertheless, the surface affinity of large halide anions is at odds with the previous understanding. By counting the number of water molecules within the first and second hydration shells of a selected ion and comparing with that in the same space of a pure water system, it is found that the halide anions, except F^- , require larger volume to solvate compared with water. Consequently, the stiffness of water is rendered as a minor problem for F^- ions residing deep inside water. In Figure 3(a), most of the water molecules in the first hydration shell of a certain anion are hydrogen-bonded with the anion. Away from the interface, the percentage of hydrogen-bonded water molecules for F^- is above 95%, the most eminent among anions. Larger anions are predicted to have more non-bonded water in their surroundings. Owing to the strong hydrogen-bond with anions, the hydrogen-bonded water is inflexible to rotate, as shown in Fig 3(b). As a result, water-water hydrogen-bonds become rare within the first solvation shells of the anions — 0.3 for F^- and 0.5 for I^- , respectively (Table S1). As displayed in Table 1, along with the loss of the solvation water at the interface, the anions strengthen the attraction with the remaining water. As F^- has the strongest attraction with hydrated water and fewer non-hydrogen-bonded water molecules, it keeps more than 5 water molecules in the first hydration shell even at the interface and is the only halide anion losing less than one water molecule, while larger anions all lose more than that.

Viewing from the energy the anions interact tightly with water and even the biggest anion, I^- , possesses a high average interaction energy with the water in the first hydration shell, $-45.6 \text{ kJ mol}^{-1}$. Nonetheless, the large energy discrepancy between the hydrogen-bonded water and non-hydrogen-bonded water is notable. The former contributes to most of the hydration energy by inserting an anion into water. In contrast, dissociating a non-bonded water can be energetically favorable, because the non-hydrogen-bonded ion-water attraction, -7 kJ mol^{-1} for I^- , is much weaker than the average water-water interaction, $-18.2 \text{ kJ mol}^{-1}$. (Fig S2 in supporting information)

Table 1. Hydration properties of ions and water

	Diameter (Å)	Volume	$N_{\text{ion}_\text{hy}1}$		$U_{\text{ion}_\text{hy}1}$ (kJ mol ⁻¹)		$U_{\text{ion}_\text{hy}2}$ (kJ mol ⁻¹)		$U_{\text{w}_\text{hy}1}$ (kJ mol ⁻¹)	
			Bulk	Interface	Bulk	Interface	Bulk	Interface	Bulk	Interface
Water	3.18	1.00	4.4	3.0					-21.5	-21.7
F ⁻	4.03	0.35	5.8	5.1	-92.8	-105.4	-5.0	-9.0	-15.9	-19.4
Cl ⁻	4.38	1.55	6.1	5.0	-65.3	-76.8	-3.4	-6.8	-17.6	-19.4
Br ⁻	4.58	1.64	6.2	5.0	-54.0	-63.3	-3.2	-6.4	-17.9	-19.3
I ⁻	4.92	2.05	6.3	4.8	-45.6	-53.7	-3.6	-4.8	-18.2	-19.3
Na ⁺	2.58	-0.12	5.7	5.3	-87.1	-86.9	-5.1	-10.4	-15.2	-19.4
K ⁺	2.93	0.15	7.1	6.5	-51.9	-52.3	-4.7	-7.8	-15.9	-19.4
Rb ⁺	3.12	0.15	8.1	7.4	-40.9	-41.2	-4.0	-6.0	-16.3	-19.4
Cs ⁺	3.53	0.53	10.2	9.0	-28.6	-29.7	-3.2	-5.2	-16.7	-19.5

* Volume is the space required for accommodating the selected ions, represented as the number of water molecules. The value is obtained by counting the difference of the number of water molecules within the first and second hydration shells of the ions from that in the same space of pure water. The negative value denotes that water becomes more condensed with more water in the same space. $N_{\text{ion}_\text{hy}1}$ is the number of water molecules in first hydration shell. $U_{\text{ion}_\text{hy}1}$ and $U_{\text{ion}_\text{hy}2}$ are the interaction energies of ions with each water molecules in the first and second hydration shell. $U_{\text{w}_\text{hy}1}$ is the interaction energy of a water molecule with its neighboring water molecule.

Going from bulk to air/water interface, ions attract both hydrogen-bonded and non-hydrogen-bonded water molecules more strongly. The length of anion-water hydrogen bond is shortened by 2%, while the non-bonded water molecules reorient towards anions as all the O-H-A (acceptor for hydrogen) angles are greater than 100°. The hydration energy of the remaining water molecules with anions increases to compensate that due to the leaving water and make the overall hydration energy larger. Because of the quick decay of the ion-water interaction, the enthalpy difference for large ions moving from bulk to interface can be approximated by the summation of the first and second hydration shell attractions. Taking advantage of the obtained data from Table 1, the enthalpy difference can readily be evaluated as

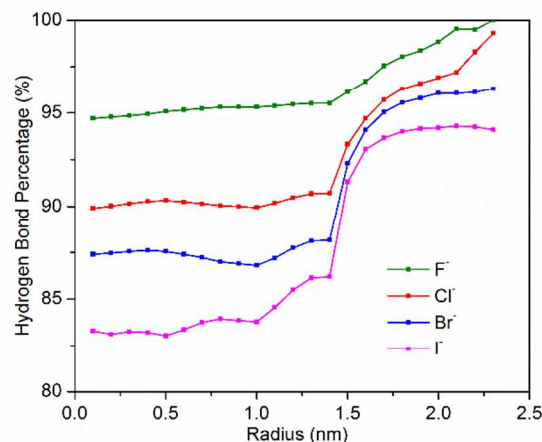
$$\Delta E = E_{\text{surface}} - E_{\text{bulk}}$$

$$E = N_{\text{ion}_\text{hy}1} \times U_{\text{ion}_\text{hy}1} + N_{\text{ion}_\text{hy}2} \times U_{\text{ion}_\text{hy}2} - V(N_{\text{w}_\text{hy}1} \times U_{\text{w}_\text{hy}1} + N_{\text{w}_\text{hy}2} \times U_{\text{w}_\text{hy}2})$$

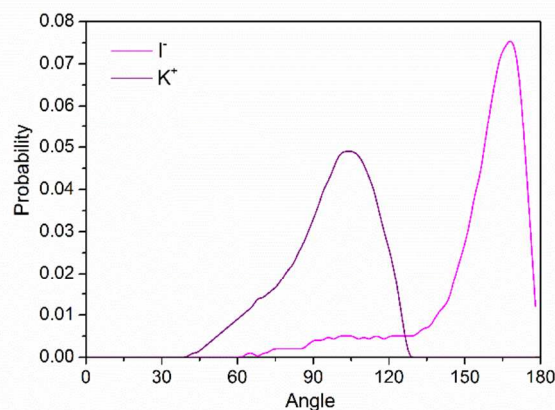
Here N denotes the number of water molecules, U is the interaction energy, V is the volume of the ion in terms of number of water molecules and the subscripts denote the specific hydration shell. The enthalpy gain of Cl⁻, Br⁻, I⁻ at the interface is approximately -19.0±3.2, -15.4±3.6 and -30.9±4.1 kJ mol⁻¹, respectively.

However, an enhancement of the ion-water interaction is not the case for cations. Albeit cations have much smaller hydration energies with water in the first hydration shell, -28.6 kJ mol⁻¹ for Cs⁺, they take advantage of a larger quantity of hydration water molecules, for example, 10.2 water molecules in the first hydration shell of Cs⁺. The water molecules solvating cations have more freedom to rotate and the H-O-X (X denotes cations) angle distributes across a wider range, as shown in Fig 3(b). Moreover, there is a proportion of water displaying the configuration that the hydrogen atom is closer to the cation than the oxygen is. Larger cations possess more steady solvation structures because of an enriched quantity of hydrogen bonds between the water molecules in the first solvation shell, for instance 4.9 water-water hydrogen bonds in the first hydration shell of Cs⁺. The enhanced hydrogen-bond network induces an opposite trend against anions as large cations are more likely caged in water. The cations are clearly not as capable of stabilizing water at the interface as anions. The total energy follows a decreasing trend when cations approach the interface

because the water leaves the hydration shells of the cations while the ion-water interaction hardly changes, as shown in Table 1.



(a)



(b)

Figure 3. (a) Percentage of water forming hydrogen bonds with the anion in the first solvation shell. (b) Rotational freedom for water in the first hydration shell of ions is represented by angular distributions of O-H- Γ^- and H-O-K $^+$.

3.4 Configurations of water

The ion specificity at interfaces is dependent on the solvent and the mechanism how water induces such discrepancy among the ions is a major concern.²¹ The average dipole moment of bulk water in a droplet is calculated as 2.53 Debye, agreeing well with previous studies.²² No specific orientation was initially observed in the bulk. However, a decreasing trend is subsequently activated when water moves towards the interfacial area. Simultaneously, water also starts to exhibit a special order, in accordance with previous studies by Ishiyama et al.²³ The positive value of the average normal component of the water dipole moment (orthogonal to the interface) presents the picture that water prefers to point hydrogen atoms towards air. The existence of a more favorable orientation of water was not only proposed at hydrophobic interface by Scatena et al.²⁴, but also accords with the long-standing interfacial electrostatic measurement that a negative potential is recorded when probes penetrate through the surface.²⁴ As an external electronic field drives the cations and anions towards opposite directions, this orientation is of importance for interpreting why anions exhibit much larger surface affinity than cations under the same conditions.

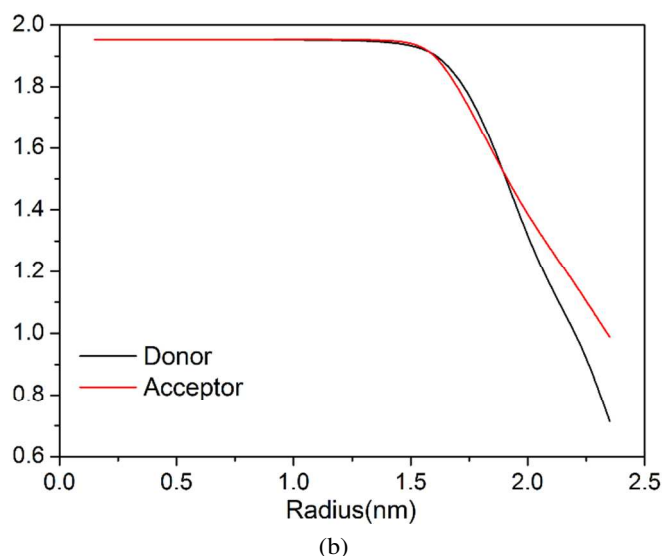
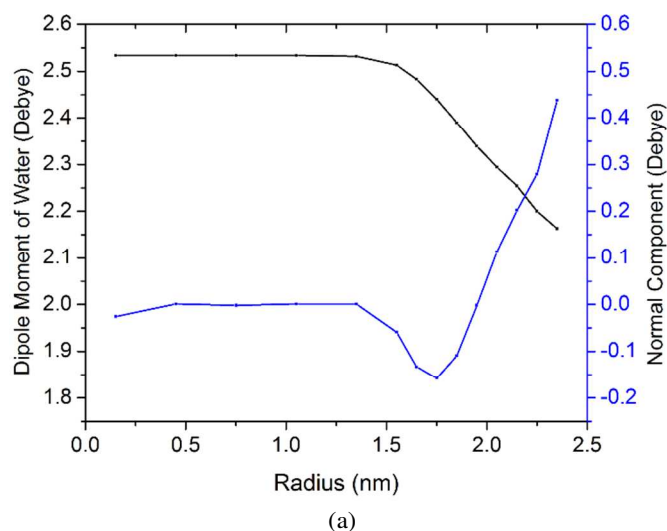
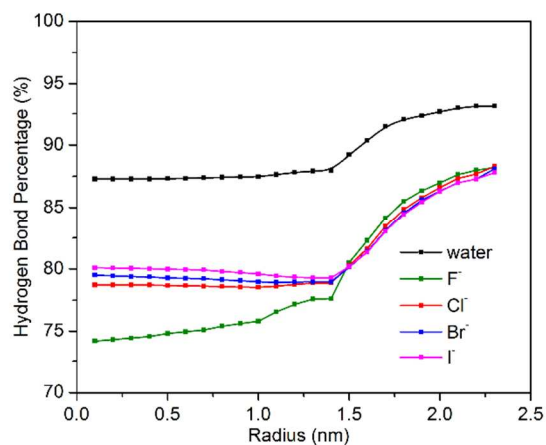


Figure 4. (a) Dipole moment (black) of water and its normal component (blue) have different trends upon approaching the interface. (b) The average number of hydrogen atoms donated and accepted per water. The normal component of the dipole moment (orthogonal to the interface) is the projection of the dipole moment on the radial vector crossing the mass center of the water.

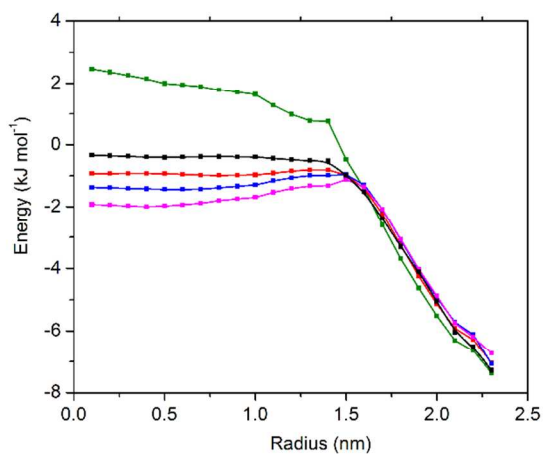
Interfacial relaxation and dangling hydrogen atoms near the surface are predicted both by spectroscopy and by ab initio simulations.²⁵ From bulk to surface, the proportion of the fully hydrated water molecules, which donate two hydrogen atoms and accept two hydrogen atoms at the same time, declines from 82.5% to 19.6%. (Fig S3 in supporting information) On the contrary, the interface is most beneficial to single-donor single-acceptor water molecules with a proportion surging to 28.7%. The acceptor-only states of water take up a substantial contribution of 14.1% of at the outermost interface, as being proposed by Wilson et al.^{25a} Water alternates its preference from donating hydrogen to accepting hydrogen. Inside the bulk, the average number of hydrogen atoms donated per water is the same as that accepted, 1.93. It is noteworthy that water accepts slightly fewer hydrogen atoms than it donates at 1.75 nm to the center of mass. The more hydrogen atoms donated by the inner water shell are absorbed by the outer layer and this is the origin for the specific order of water. This tendency is then reversed right at the interface, resulting in more free hydrogen atoms than oxygen atoms above the interface. More free hydrogen atoms dangling at the interface are also an attraction for anions to stay there.

Upon addition of ions into water, the interesting picture emerges that all the ions studied are capable of breaking the water-water hydrogen bonds, leading to a reduced hydrogen bonded percentage of water, from 87% to less than 80% for the larger anions. For F $^-$, the number further decreases to 75%, as seen in Fig 5(a). The strengthened water-water hydrogen bond by the prominent surface is weakened as well, with the energy dropping from 24.5 kJ mol $^{-1}$ to 22.3 kJ mol $^{-1}$, though the hydrogen bond lifetime is slightly prolonged (Table S1 in supporting information). In this respect, the structure-building argument is only appropriate for hydrogen bonds between ion and water, but not for the water-water hydrogen bonds. Fluoride anions exhibit another intriguing outcome as they evidently disrupt the water-water hydrogen bonds. The non-bonded water shall be repelled from the first solvation shell of water owing to a positive hydration energy, as shown in Figure 5. This implies that water molecules are destabilized in the bulk

and reach the interface more readily. Regarding the total water-water interaction within the first and second hydration shells, the energy barrier for water to reach the interface is 3.05 kJ mol^{-1} in the presence of F^- . The stimulated affinity of water to the surface indicates that, unlike the larger anions, F^- does not reside at the interface. At the same time, the effects that the different cations play on water are hard to distinguish, as those effects are quite limited for cations.



(a)



(b)

Figure 5. Effect of ions on water structure. (a) Percentage of hydrogen bonds formed by a water molecule with its neighboring water molecules. (b) Non-hydrogen-bonded energy between two adjacent water molecules.

4. Conclusions

The extensive correlations between the prevalence of ions in water clusters and atmospheric relevant phenomena necessitate a better understanding of the origin of ion specificity. In this study, a series of complex water clusters was investigated in order to study the mechanism for anions to reach the interface and change the surrounding environment. While larger halide anions are found to reach their preferred interface promptly,

showing a distinct interfacial propensity, the distribution of cations depends on their counterions. In the presence of large halide anions, they tend to abound somewhat beneath the interface, in contrast to anions which clearly show preference to reside at the interface. The combined effects of size and polarization pull the anions to the interface where they indeed are energetically more favorable than the corresponding cations. Non-hydrogen-bonded moieties around anions are relatively weakly attracted, thereby more easily losing water in the hydration shell, while hydrogen-bond networks are more stable in the vicinity of large cations. That the near-surface water molecules prefer to point out their hydrogen atoms towards the air induces a directing electronic field, which is advantageous for the interfacial propensity of anions. We infer that the joint effect of hydration structure and water orientation is the reason for the discrepancy of ionic interfacial propensity while cations show less surface affinity even with the same size and polarization as those of the anions. Despite the notably large ion-water interactions, ions weaken the original water-water attraction, contradicting with the debatable assertion of building water structure. Hereby, we contend that, besides size and polarization of the ions, the water orientation and the free dangling water at the interface are of great importance to understand the surface affinity and characteristic of ions, and that the conventional kosmotrope must be better defined. The present atomistic study thus supports a more sophisticated understanding of ion-water interactions and the active involvement of ions in aerosol formation and heterogeneous reactions.

Acknowledgements

The authors thank the Swedish Infrastructure Committee (SNIC) for providing computational resources for the project “Multi-physics Modeling of Molecular Materials”, SNIC2013-26-31. L.S. thanks the China Scholarship Council for financial support.

Notes and references

Corresponding Author
agren@theochem.kth.se

^a Department of Theoretical Chemistry and Biology, School of Biotechnology, Royal Institute of Technology, S-10691 Stockholm, Sweden

Electronic Supplementary Information (ESI) available: Supplementary hydration properties, distribution of Li^+ , snapshots of MD simulations, distribution of Cl^- with attenuated polarizations, influence of cations on water, water donor-acceptor states are listed in supporting information. This material is available free of charge via the Internet at <http://pubs.acs.org>.

- 1 L. Onsager and N. N. T. Samaras, *J. Chem. Phys.*, 1934, **2**, 528-536.
- 2 D. J. Tobias, A. C. Stern, M. D. Baars, Y. Ilevin and C. J. Mundy, *Annu. Rev. Phys. Chem.*, 2013, **64**, 339-359.
- 3 a) P. Jungwirth and D. J. Tobias, *J Phys Chem B*, 2001, **105**, 10468-10472; b) C. Caleman, J. S. Hub, P. J. van Maaren and D. van Spoel, *P Natl Acad Sci USA*, 2011, **108**, 6838-6842; c) S. Ghosal, J. C. Hemminger, H. Bluhm, B. S. Mun, E. L. D. Hebenstreit, G.

- Ketteler, D. F. Ogletree, F. G. Requejo and M. Salmeron, *Science*, 2005, **307**, 563-566; d)D. F. Liu, G. Ma, L. M. Levering and H. C. Allen, *J Phys Chem B*, 2004, **108**, 2252-2260; e)U. Kaatz, *J Solution Chem*, 1997, **26**, 1049-1112.
4. W. R. Simpson, R. von Glasow, K. Riedel, P. Anderson, P. Ariya, J. Bottenheim, J. Burrows, L. J. Carpenter, U. Friess, M. E. Goodsite, D. Heard, M. Hutterli, H. W. Jacobi, L. Kaleschke, B. Neff, J. Plane, U. Platt, A. Richter, H. Roscoe, R. Sander, P. Shepson, J. Sodeau, A. Steffen, T. Wagner and E. Wolff, *Atmos Chem Phys*, 2007, **7**, 4375-4418.
 5. L. M. Pegram and M. T. Record, *J Phys Chem B*, 2007, **111**, 5411-5417.
 6. D. J. Tobias and J. C. Hemminger, *Science*, 2008, **319**, 1197-1198.
 7. R. Zangi, *J Phys Chem B*, 2010, **114**, 643-650.
 8. S. J. Stuart and B. J. Berne, *J Phys Chem-U.S.*, 1996, **100**, 11934-11943.
 9. Y. Marcus, *Chem Rev*, 2009, **109**, 1346-1370.
 10. a)L. Sun, X. Li, T. Hede, Y. Q. Tu, C. Leck and H. Agren, *J Phys Chem B*, 2012, **116**, 3198-3204; b)Y. Zhao, H. Li and X. C. Zeng, *J Am Chem Soc*, 2013, **135**, 15549-15558.
 11. L. X. Dang and D. E. Smith, *J Chem Phys*, 1993, **99**, 6950-6956.
 12. J. Noah-Vanhoucke and P. L. Geissler, *P Natl Acad Sci USA*, 2009, **106**, 15125-15130.
 13. a)E. Guardia, I. Skarmoutsos and M. Masia, *J Chem Theory Comput*, 2009, **5**, 1449-1453; b)J. M. Heuft and E. J. Meijer, *J Chem Phys*, 2003, **119**, 11788-11791; c)J. M. Heuft and E. J. Meijer, *J Chem Phys*, 2005, **123**; d)S. Raugei and M. L. Klein, *J Chem Phys*, 2002, **116**, 196-202.
 14. M. J. Krisch, R. D'Auria, M. A. Brown, D. J. Tobias, J. C. Hemminger, M. Ammann, D. E. Starr and H. Bluhm, *J Phys Chem C*, 2007, **111**, 13497-13509.
 15. a)H. J. C. Berendsen, D. Vandespoel and R. Vandrunen, *Comput Phys Commun*, 1995, **91**, 43-56; b)B. Hess, C. Kutzner, D. van der Spoel and E. Lindahl, *J Chem Theory Comput*, 2008, **4**, 435-447; c)E. Lindahl, B. Hess and D. van der Spoel, *J Mol Model*, 2001, **7**, 306-317; d)D. Van der Spoel, E. Lindahl, B. Hess, G. Groenhof, A. E. Mark and H. J. C. Berendsen, *J Comput Chem*, 2005, **26**, 1701-1718.
 16. a)G. Lamoureux, A. D. MacKerell and B. Roux, *J Chem Phys*, 2003, **119**, 5185-5197; b)G. Lamoureux and B. Roux, *J Phys Chem B*, 2006, **110**, 3308-3322.
 17. a)S. Nose, *Mol Phys*, 1984, **52**, 255-268; b)W. G. Hoover, *Phys Rev A*, 1985, **31**, 1695-1697.
 18. a)T. Darden, D. York and L. Pedersen, *J Chem Phys*, 1993, **98**, 10089-10092; b)U. Essmann, L. Perera, M. L. Berkowitz, T. Darden, H. Lee and L. G. Pedersen, *J Chem Phys*, 1995, **103**, 8577-8593.
 19. J. S. Hub, B. L. de Groot and D. van der Spoel, *J Chem Theory Comput*, 2010, **6**, 3713-3720.
 20. Y. Levin, *Phys. Rev. Lett.*, 2009, **102**, 147803.
 21. C. Calero, J. Faraudo and D. Basto-Gonzales, *J. Am. Chem. Soc.*, 2011, **133**.
 22. a)J. K. Gregory, D. C. Clary, K. Liu, M. G. Brown and R. J. Saykally, *Science*, 1997, **275**, 814-817; b)T. R. Dyke, K. M. Mack and J. S. Muentner, *J Chem Phys*, 1977, **66**, 498-510.
 23. I. T. and M. A., *J. Phys. Chem. Chem*, 2006, **111**, 721-737.
 24. a)L. F. Scatena, M. G. Brown and G. L. Richmond, *Science*, 2001, **292**, 908-912; b)A. Frumkin, *Z. Phys. Chem.*, 1924, **34**.
 25. a)K. R. Wilson, B. S. Rude, T. Catalano, R. D. Schaller, J. G. Tobin, D. T. Co and R. J. Saykally, *J Phys Chem B*, 2001, **105**, 3346-3349; b)K. R. Wilson, R. D. Schaller, D. T. Co, R. J. Saykally, B. S. Rude, T. Catalano and J. D. Bozek, *J Chem Phys*, 2002, **117**, 7738-7744; c)I. F. W. Kuo and C. J. Mundy, *Science*, 2004, **303**, 658-660.